Proceedings of
11th European Conference on Turbomachinery Fluid dynamics & Thermodynamics
ETC11, March 23-27, 2015, Madrid, Spain

NUMERICAL SIMULATION OF ACOUSTIC LINERS IN NACELLE TURBOFANS TOWARDS AIRCRAFT NOISE REDUCTION

T. Deconinck - S. Vilmin – P. Ferrante – C. Hirsch

NUMECA International, Brussels, Belgium, thomas.deconinck@numeca.be

ABSTRACT

An innovative technique is presented to reduce noise from turbofan aircraft engines by incorporating the acoustic treatment with liners in engine ducts. The tonal noise source and the near field sound propagation in the nacelle duct are simultaneously predicted with a single CFD analysis based on an efficient Nonlinear Harmonic (NLH) method. The wall acoustic impedance has been incorporated in the NLH module of the solver and effectively damps the acoustic pressure fluctuations by a factor corresponding to the measured impedance. The sound radiation to the far field is computed with the Green's function approach implemented in a Boundary Element Method (BEM) frequency domain solver of the convective Helmholtz equation. The approach has been validated through various test cases, including a comparison with experimental results from the Grazing Incidence Tube at the NASA Langley Research Center. This approach has also been applied to the simulation of the ANCF (Advanced Noise Control Fan) engine developed at the NASA Glenn Research Center for the cases with and without liner.

NOMENCLATURE

$\tilde{p}$	Wall pressure fluctuations
r	Acoustic resistance
$\tilde{v}_n$	Wall normal velocity fluctuations
χ	Acoustic reactance
Z	Acoustic impedance
AAPL	Aero-Acoustic Propulsion Laboratory
ANCF	Advanced Noise Control Fan
BEM	Boundary Element Method
CAA	Computational Aero Acoustics
CFD	Computational Fluid Dynamics
CFL	Courant-Friedrichs-Lewy
CROR	Counter-Rotating Open Rotor
FAR	Federal Aviation Regulations
FE	Finite Element
GIT	Grazing Incidence Tube
ICAO	International Civil Aviation Organization
NLH	Nonlinear Harmonic (method)
OGV	Outlet Guide Vanes
RANS	Reynolds-Averaged Navier-Stokes

INTRODUCTION

Aircraft engine fan noise is a major contributor to noise emissions at take-off and landing. In order to increase the community acceptance of aircraft transportation and ensure at the same time the satisfaction of the certification rules (FAR, ICAO), it is mandatory to develop low noise

techniques, such as acoustic liners. Predicting the impact of those liners on the noise levels of aircrafts is an essential element in designing aero-engines with affordable computational cost [1].

The optimization of the power plant components requires the adoption of a multidisciplinary approach in the application of CFD and CAA computational models to accurately predict the engine noise emissions. The application of CAA to predict acoustic propagation and absorption in turbofan ducts has been reviewed by Astley et al. [2] and they proposed liner optimization procedures based on frequency-domain Helmholtz FE methods. In this article, we focus on the applications of computational models to evaluate the effect of acoustic treatment with the potential benefit of using those models for reliable design purposes.

Liners are characterized by boundaries with specified values of impedances and an increased understanding of liner effects on sound propagation is required. Traditionally, the presence of a mean flow with a boundary layer has been accounted for through the Ingard [3] or the Myers [4] boundary condition. It is shown that a direct use of the nominal impedance for the acoustic liner is justified if the mean flow is accurately accounted for by the flow equations [5]. Jones et al. [6] provided an extensive database acquired using the NASA Langley Research Grazing Incidence Tube (GIT).

In this paper an innovative integrated “CFD-acoustic” computational approach is applied to the simulation of acoustic liners for the GIT test case and for the Advanced Noise Control Fan (ANCF), developed at the NASA Glenn Research Center [7]-[8]. For this later case, the computational approach includes the full coupling of automatic mesh generation for complex 3D geometries, the simultaneous CFD analysis of the acoustic source domain and of the sound propagation in the nacelle duct in the near-field, followed by the final radiation analysis to obtain the noise in the far-field. The approach is based on the exploitation of three main key ingredients: 1) an efficient CFD solver based on the Non Linear Harmonic (NLH) method [9]-[10] capable to predict at affordable cost the unsteady flow field generated and propagated by the fan; 2) an integrated “liner-type” boundary in the CFD solver that is characterized by its impedance, which is a frequency-dependent complex function for which the real and imaginary parts relate to the resistance and reactance, respectively; 3) an efficient frequency domain aeroacoustic tool performing the far-field radiation analysis by means of the Green’s function approach implemented in a Boundary Element Method (BEM) solver.

The first section of this paper describes the simulation approach adopted for the CFD simulations with the NLH method and the acoustic liner as well as for the CAA simulations with the BEM code. The second section provides details on the validation test case, i.e. the grazing incidence tube (GIT) at NASA Langley Research Center. The results obtained for the Advanced Noise Control Fan (ANCF) are discussed in section three. Comparisons with the available experimental data are provided in section two and three. The capability of the integrated simulation tool to model successfully the whole computational chain is finally assessed in the conclusive section.

SIMULATION SETUP

Nonlinear Harmonic (NLH) Method

The NLH approach [9]-[10] can be considered as a bridge between classical steady state and full unsteady calculations, providing an approximate unsteady solution at reduced calculation costs. The unsteady flow perturbation is Fourier decomposed in time, and by a casting in the frequency domain, transport equations are obtained for each time frequency. The user controls the accuracy of the unsteady solution through the order of the Fourier series. Alongside the solving of the time-averaged flow steady-state equations, each frequency requires the solving of two additional sets of conservation equations (for the real and imaginary parts of each harmonic).

The method is made nonlinear by the injection of the so-called deterministic stresses, resulting from all the solved frequencies, into the time-averaged flow solver. In the same way as the Reynolds stresses represent the totality of the influence of the turbulent fluctuations on the mean flow, the deterministic stresses which appear in the time-averaged equations as time-averaged

products of unsteady fluctuations, represent the full nonlinear effects of the flow unsteadiness on the time-averaged flow. In this case, the closure of the model is obtained by calculating the deterministic stresses directly from the harmonic solutions, which is an important advantage as it provides an improved time averaged flow solution, incorporating all the effects of the unsteadiness.

Because of the transposition to the frequency domain, only one blade channel is required like a steady flow simulation. The method also features a treatment that enhances the flow continuity across the rotor/stator interface by a reconstruction of the harmonics and the time-averaged flow on both sides of the interface. A non-reflective treatment is applied as well at each interface.

The NLH methodology has been successfully applied in the past to an integrated aero-engine including fan, OGV and nacelle intake in presence of ground effects and crosswind conditions [11]. More recently the methodology has been extended to fully account for installation effects of pylons/nacelles on CROR aerodynamics and noise [12]. The NLH method provides more accuracy in comparison to the classical solution of the Convective Wave Equation [13] keeping into account the full nonlinear effects of the flow unsteadiness on the time-averaged flow solution and by simulating the propagation of the acoustic waves inside the boundary layer and across shear layers.

Impedance Boundary Condition

The NLH method, implemented in the FINE^{TM}/Turbo CFD software, enables the simultaneous simulation of the tonal noise generation and propagation in the nacelle duct, also in presence of acoustic liners. It provides with one single analysis the unsteady flow solution usable for the characterization of the aerodynamic performance and the tonal noise signature of the fan. The direct use of the nominal impedance, without the use of Ingard [3] or the Myers [4] boundary condition is justified since the mean flow is properly accounted for in the NLH method. The nominal impedance of the liner can be used as a boundary condition when the boundary layer is resolved.

The impedance boundary condition is given by

$$\tilde{v}_n = v_{nR} + I v_{nI} = \frac{\tilde{p}}{Z} \tag{1}$$

where $\tilde{v}_n$ and $\tilde{p}$ are the wall normal velocity fluctuations and the wall pressure fluctuations, respectively. The impedance is of the form

$$Z = r + I\chi \tag{2}$$

where the real part, r, is the resistance and the imaginary part, χ, is the reactance. The resistance is related to the dissipation of energy when the sound wave impinges on the liner surface, and the reactance is related to the phase shift of the reflected wave. Modeling the flow along a wall covered with an acoustic liner results in the computation of a normal velocity fluctuation given by

$$v_{nR} = \frac{r\,p_R + \chi\,p_I}{r^2+\chi^2};\; v_{nI} = \frac{r\,p_I - \chi\,p_R}{r^2+\chi^2} \tag{3}$$

The pressure perturbation in the cell closest to the wall is used as an approximation of the wall pressure. For a given frequency, the acoustic impedance is assumed to be constant along the liner and the treatment is assumed to be impermeable, meaning that the normal component of the time-mean velocity remains zero.

Integrated Acoustic Solver (BEM)

The far-field acoustic radiation analysis is performed with the Green's function approach implemented in the Boundary Element Method (BEM) module of FINE^{TM}/Acoustics [13]. This latter is an aero- and vibro-acoustic suite, fully integrated with the CFD software, including also a Finite Element Method (FEM) solver of the Pierce-Howe equation [14] and a Ffwocs Williams-Hawkings (FW-H) solver [15]. The communication between the acoustic computational suite and the CFD software is done in the native CFD format, reading directly the harmonic data computed by the NLH solver.

GRAZING INCIDENCE TUBE

Test case description

The test case considered in this section is the grazing incidence tube (GIT) at NASA Langley Research center [6]. As shown in fig.1, the tube has internal dimensions of 0.812 m × 0.051 m × 0.051 m and contains an axially-centered liner of 0.406 m length which we model with a uniform impedance. The source and exit planes of the duct are located at $x = 0$ and $x = 0.812$ m, respectively, and the two side walls and lower wall of the duct are rigid. We will compare the acoustic pressure field on the wall opposite the liner with acoustic measurements at a set of discrete locations. The liner used in the experiment is a ceramic tubular liner (CT57) which consists of parallel, cylindrical channels embedded in a ceramic matrix.

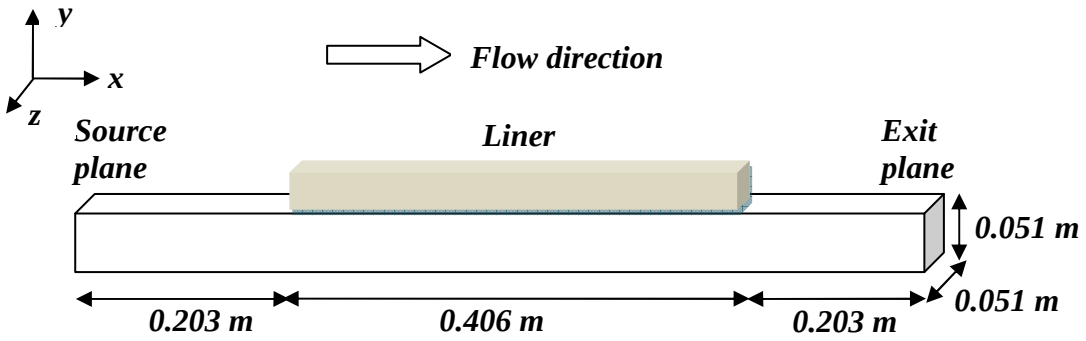

Figure 1: Sketch of the grazing flow incidence tube test section

For this test case, plane waves are introduced through the inlet together with a mean flow of average Mach 0.335 over the liner. Normalized impedance values of the liner are given by Jones et al. [6] in Table 1 for frequencies ranging from 500 to 3000 Hz. In our computations, the exit plane is simulated as an outlet boundary condition with perfect anechoic properties. We do therefore not exactly reproduce the proposed test case with exit impedance boundary conditions causing some reflections.

f, Hz	*500*	*1000*	*1500*	*2000*	*2500*	*3000*
r	*0.75*	*0.19*	*1.18*	*4.93*	*0.92*	*0.73*
χ	*-0.57*	*0.15*	*1.31*	*-1.95*	*-1.39*	*-0.22*

Table 1: Normalized liner impedances educed using Q3D-FEM from Jones et al. [6] with $M_0 = 0.335$

Results and discussion

The Nonlinear Harmonic (NLH) method has been integrated with the impedance boundary condition to simulate the grazing incidence tube. The CFD code solves the compressible flow equations in conservative form on multi-block structured meshes. Computations have been performed for Euler and Navier-Stokes flows, and adequate resolutions have been obtained with meshes consisting of 256×16×16 cells and 289×81×81 cells, respectively. In the latter case, the y^+ was found not to exceed 5 throughout the solid boundaries. We verified the implementation of the acoustic impedance by comparing the acoustic results evaluated with the Euler solver of FINE^{TM}/Turbo and FEM solver of FINE^{TM}/Acoustics and a perfect agreement between the two codes has been confirmed for the uniform flow case.

The Reynolds-averaged Navier-Stokes (RANS) equations were solved with the Spalart-Allmaras turbulence model and with the k-ω shear stress transport model. Since no significant differences were observed between the two models in terms of sound pressure levels, the Spalart-Allmaras turbulence model was used for the presented results. To accelerate the convergence to steady state, a local time step is used with a given Courant-Friedrichs-Lewy (CFL) number of 3.

Figure 2 and figure 3 show the sound pressure levels and phase results for the test case with average Mach number $M_0 = 0.335$. In these plots, we compare the numerical results obtained from the Euler and Navier-Stokes solvers using the NLH method with the experimental data from Jones et al. [6]. Even though an Ingard [3] or Myers [4] boundary condition should ideally be used for the Euler solver with uniform flow to take into account the boundary layer, we selected the same nominal impedance of the liner for the Euler and Navier-Stokes test cases.

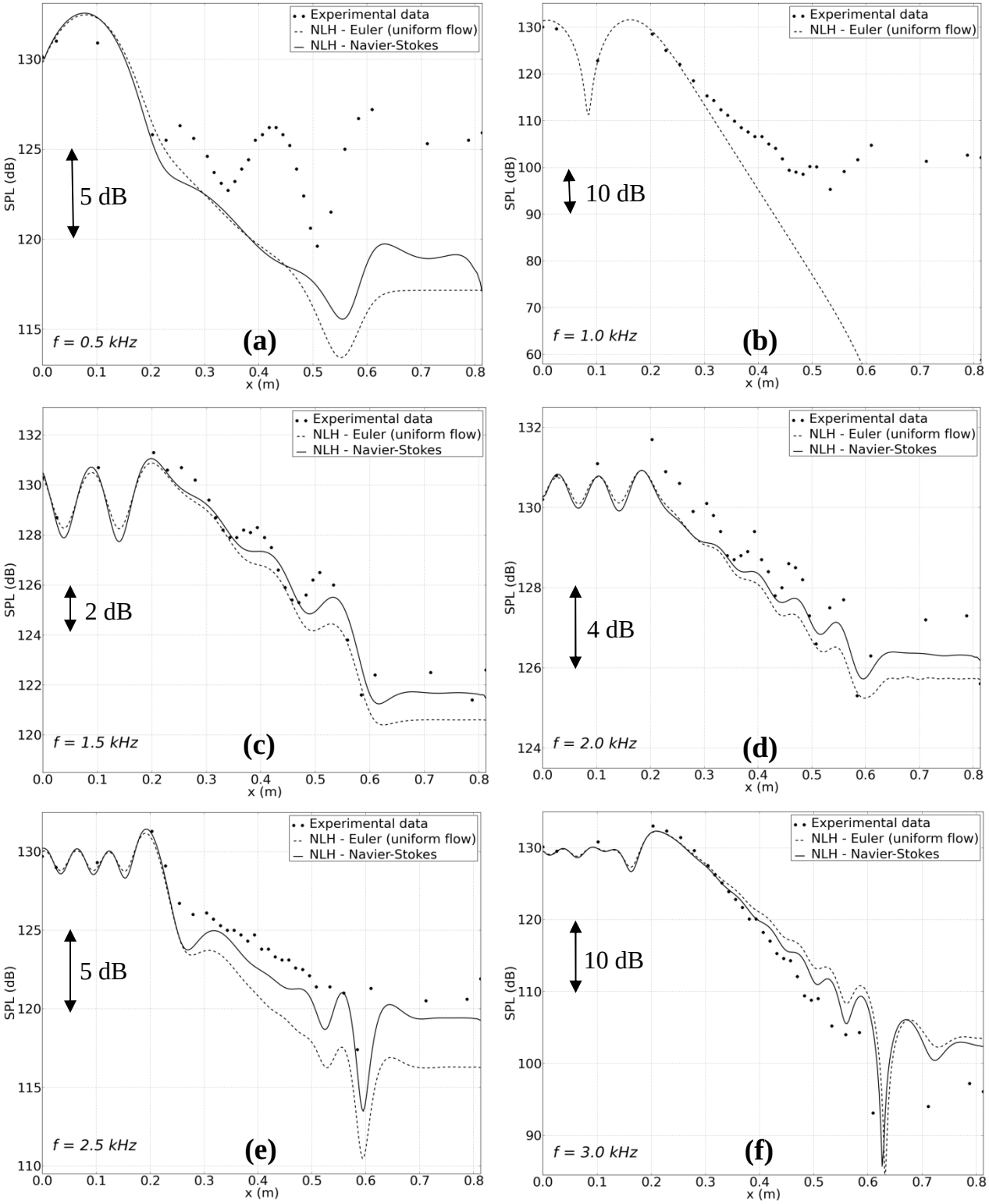

Figure 2: Sound pressure levels results for mean flow $M_0 = 0.335$ (experimental data from Jones et al. [6])

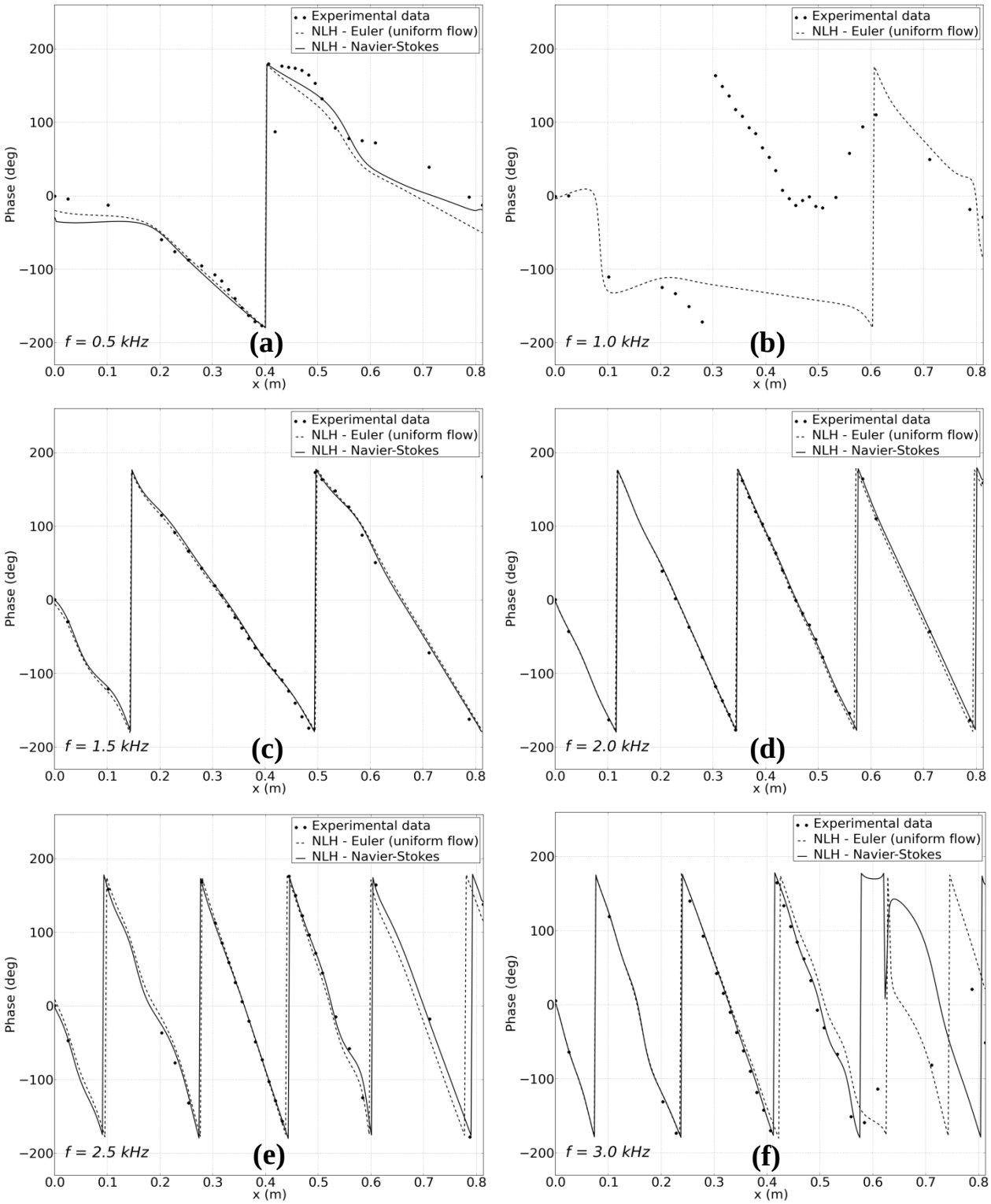

Figure 3: Phase results for mean flow M_0 = 0.335 (experimental data from Jones et al. [6])

The same inlet boundary condition with uniform flow was used for the Euler and Navier-Stokes test cases. We initially performed a set of simulations with prescribed flow profiles at the inlet to mimic the measured flow profiles at the axial position located at x=0.2032 from the inlet. We did not observe significant differences or improvements with the prescribed velocity profiles for the Navier-Stokes solver, and kept the uniform flow profile at the inlet boundary condition with its natural boundary layer development through the domain. We did not manage to obtain a converged

Navier-Stokes solution for the test case with large acoustic damping (f = 1 kHz), even after reducing the CFL number and this probably has to do with the flow instability encountered by Burak et al. [5] for this frequency (see figures 2(b) and 3(b)).

The overall impression given by the results for the sound pressure levels is that the methods are capable of predicting the effects of the liner quite well, with the Navier-Stokes solver giving in general more accurate results than the Euler solver. The largest discrepancies in terms of sound pressure levels are found to occur near the two lowest frequencies (see figures 2(a) and 2(b)). One reason may be the outlet boundary condition that does not take into account the acoustic reflections which should be captured with a nominal exit impedance. An increase in SPL values in the duct would result from this modified boundary condition.

The agreement of the results for the phase angles is good, except for the cases with important damping downstream of the liner (see figures 3(b) and 3(f)). We could not present Navier-Stokes results for the test case with f = 1 kHz because of a flow instability.

ADVANCED NOISE CONTROL FAN

Test case description

The Advanced Noise Control Fan (ANCF) is a 1.2 m diameter ducted fan (see figure 4) used for aerodynamic and aeroacoustic measurements. The ANCF is located in the Aero-Acoustic Propulsion Laboratory (AAPL) at the NASA Glenn Research Center [7]-[8]. The ANCF configuration considered in this section corresponds to a rotor of 16 blades with a pitch angle of 28° and to a set of 14 stator vanes located at 1-chord spacing downstream of the fan. The fan rotates at a speed of 1800 RPM resulting in a tip speed of 114 m/s and in an inlet duct Mach number of ~ 0.15. The fundamental blade passing frequency (BPF) is 480 Hz.

(a) **(b)**

Figure 4: Overview of the ANCF (a). ANCF installed rotor blades (b) [7]- [8]

The domain considered in the computation includes the whole nacelle duct, the lip and the near field. Compared to full unsteady 360° sliding grid computations, the number of mesh points is greatly reduced as only one blade passage is meshed. As shown in figure 5(a), the near-field is bounded by a permeable “external” surface located in front of the nacelle intake. A numerical simulation will be performed with a liner in the nacelle which is illustrated in figure 5(b).

The CFD mesh has been generated with AutoGrid5^{TM}, the NUMECA Int. automatic hexahedral structured grid generator. This tool allows to easily and rapidly mesh any kind of rotating machinery, providing a computational mesh suitable for the CFD computation of the unsteady flow field in the fan region and for the simultaneous analysis of the sound propagation in the nacelle duct and in the nacelle near-field.

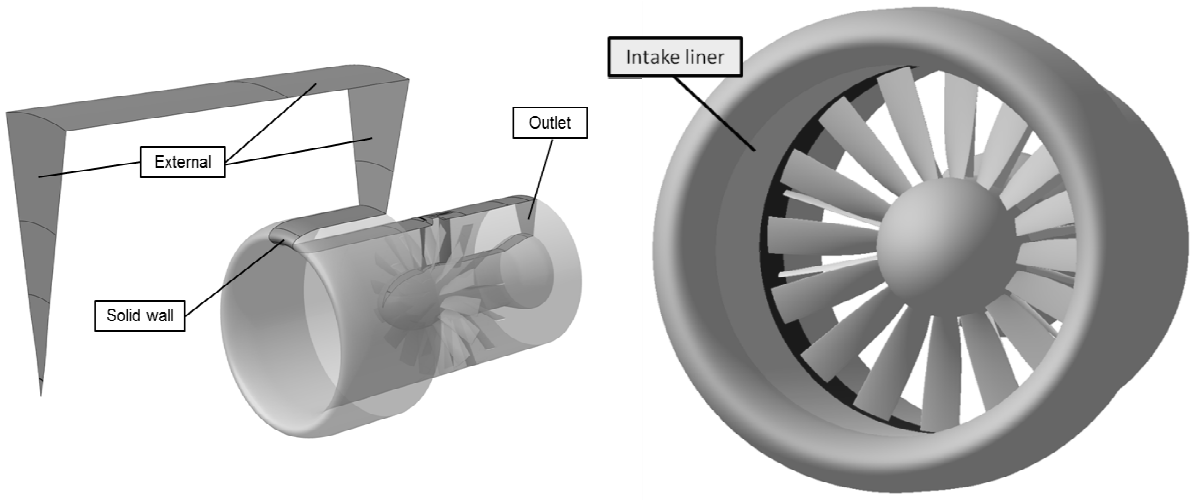

(a) **(b)**

Figure 5: Overview of the computational domain (a). Solid boundaries with liner (b).

As shown in figure 6(a), 97 flow paths are used in the main channel for the rotor blade (including 17 in the shroud tip gap), 81 flow paths are used in the main channel for the stator vane. Only one interblade channel per row is meshed, representing a sector of 25.71° for the stator domain (periodicity 14) and 22.5° for the rotor domain (periodicity 16). As shown in figure 6(b), a O4H topology is used with a skin block around the blades and 4 H blocks around it. This blade-to-blade topology is extended in the tip gap for the rotor blade. The inlet bulb is meshed with a butterfly topology to avoid a singular line at the zero radius line. The mesh fulfills all the usual quality criteria in terms of mesh smoothness and regularity. The generated mesh is characterized by nearly uniform elements in the nacelle duct and in the nacelle near-field, with a maximum element size of 40 mm that guarantees a spatial resolution at the maximum frequency (3*BPF = 1440 Hz) of 10 points per wavelength. The mesh is composed of 8 million nodes.

The turbulence is modeled by the one-equation Spalart-Allmaras model, with y^+ not exceeding 10 on the first layer of cells above the solid surfaces. For the harmonic simulation, 3 harmonics are considered for each perturbation. This number has been chosen to obtain a reasonable trade-off between the accuracy of the calculation and the computational effort. In this study no sensitivity analysis has been performed with respect to the number of the harmonics considered but validations have shown that 3 harmonics provide an excellent representation of the full unsteady solution [16]. To increase the convergence speed, a full multigrid strategy is used with 4 grid levels.

Once the NLH computation is performed, the sound radiation to the far field is computed with the Green's function approach implemented in the BEM frequency domain solver of the convective Helmholtz equation. In this type of simulation the flow field is considered uniform in the whole radiation domain. The radiating surface mesh and the relative harmonics of the acoustic pressure and the acoustic velocity distributions are automatically extracted from the external boundary of the NLH mesh (figure 7) and used to start the radiation analysis. The noise levels are finally computed at the virtual microphones located in the far-field.

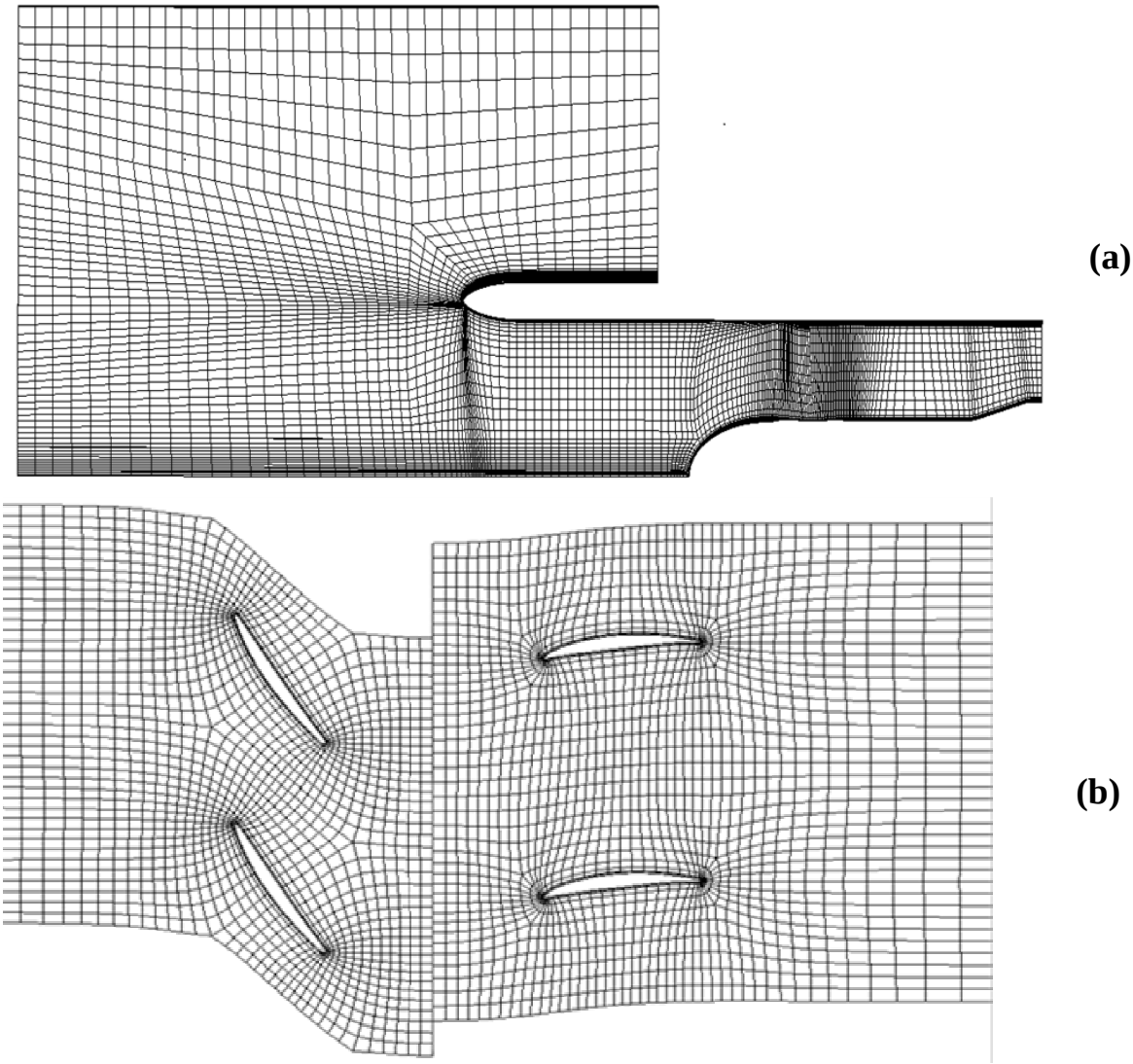

Figure 6: Meridional view of the mesh (a). Blade-to-blade view of the mesh (b). The coarse grid level 222 is selected to improve the visualization.

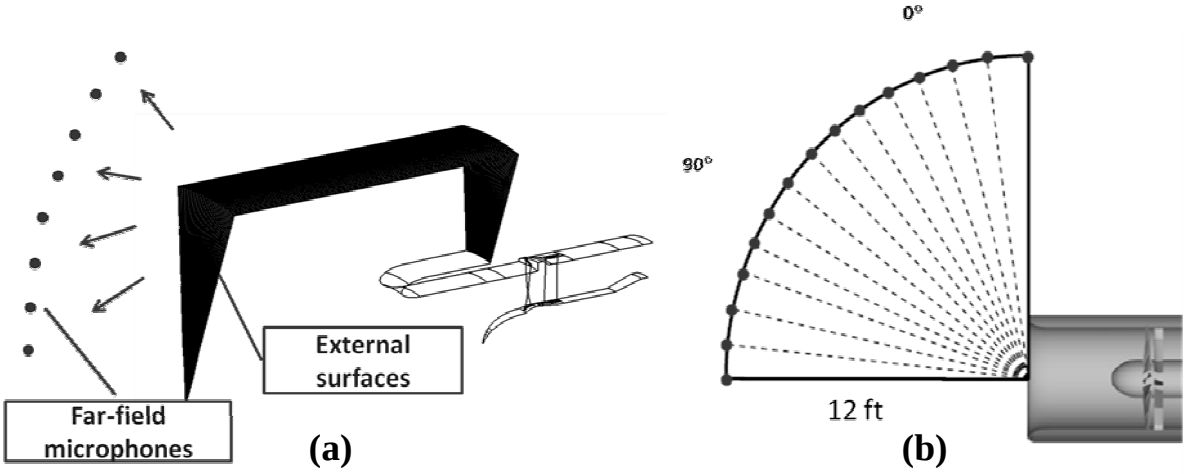

Figure 7: Far-field microphones with radiating external surfaces

Results and discussion

The aerodynamic results for the base case without liner have been documented in Ferrante et al. [1] and will not be reproduced. This paper concentrates on the aeroacoustic results since the liner

has little influence on the aerodynamic flow fields. We do not have experimental data to compare with for the case with liner and will use an arbitrary impedance value, representative of typical liner configurations installed in turbofan engine nacelles. For simplification purposes, a constant normalized value of the impedance with resistance $r = 2$ and reactance equal $\chi = -0.5$ was selected independently of the harmonic frequencies. As shown in figure 8, the presence of the liner considerably reduces the harmonic pressure fluctuations within the duct and in the near-field. This reduction is observed for all three harmonics. It should be noted that this liner is idealized since the damping is normally effective for one particular frequency with impedance values that depend on the frequencies.

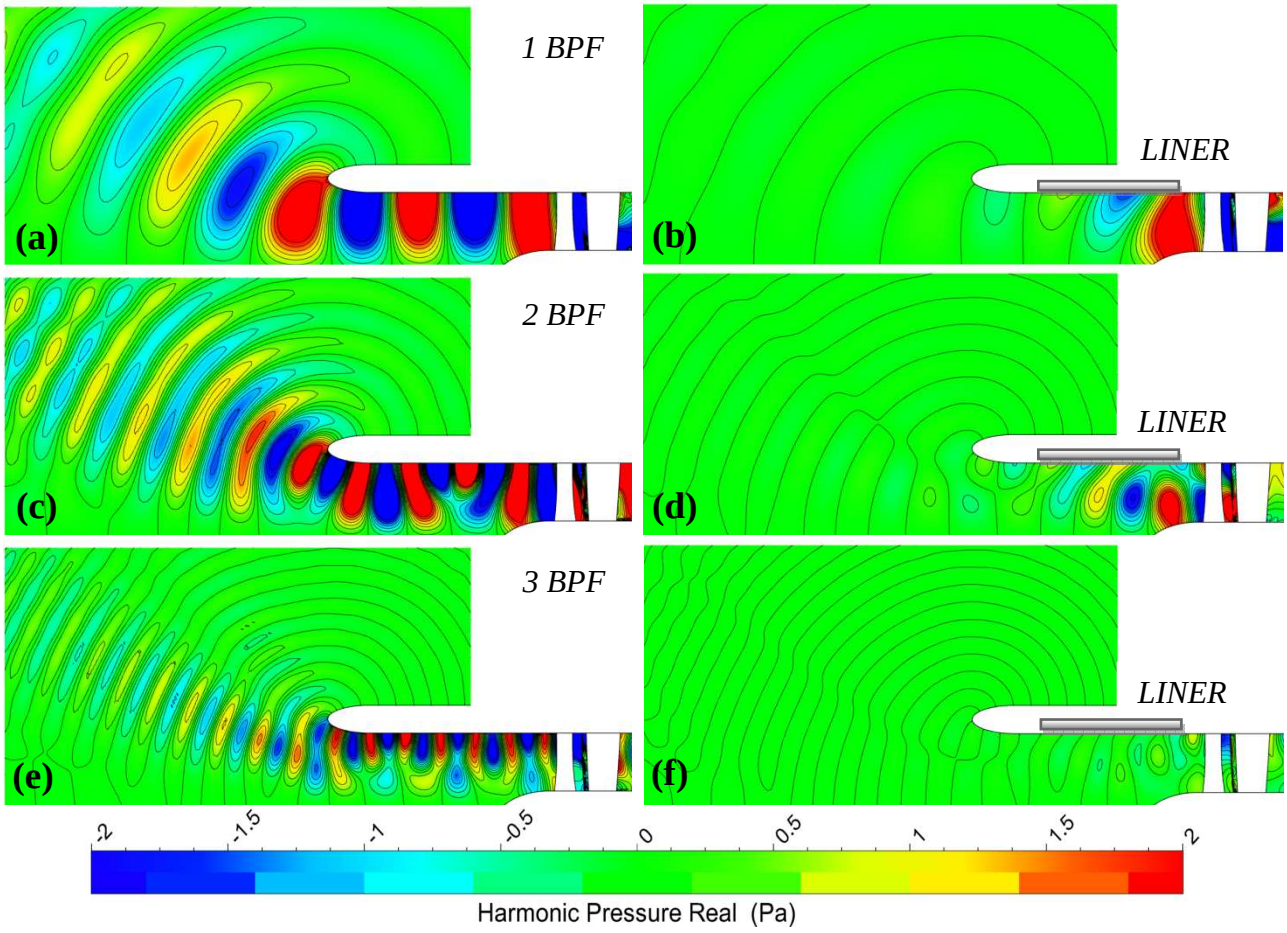

Figure 8: Pressure fluctuation contour plots

Figure 9 shows the comparison of the far-field directivities obtained at the three blade passing frequencies. The sound directivity in the far-field is dominated by rotor-stator interaction noise. The sound waves (duct modes) associated with this type of noise propagate with a given angle with respect to the engine axis, contributing to the noise peak observed in the angular range between 30° and 40° [17]-[18]. For the case without liner, the noise peak is quite accurately predicted in amplitude and angle. As shown in figure 9(a), a very good agreement is obtained in the angular range above 10° and below 75° for the first blade passing frequency. A slight under-prediction of maximum 5 dB is highlighted at the highest angles, while a large deviation from the experimental data is observed on the fan axis (0°). Figure 9(b) reports the results obtained at the second harmonic for the case without liner. In the angular range 15°-45° the numerical prediction is well in line with the experimental evidence. The maximum SPL of the noise generated by the fan is reproduced within 2 dB, while the angle of maximum radiation is slightly under-predicted of 5°. For the third harmonic (see figure 9(c)), the noise peak is well predicted in amplitude (85 dB) while the under-prediction at low and high angles is still observed.

The generation mechanism of noise at low angles observed in the NASA experiments is likely due to azimuthal irregularities in the investigated nacelle configuration. Such irregularities are difficult to include in the simulation, as their precise features are not known precisely. The other discrepancies observed at high microphones angles might be explained by the combination with noise radiated from the bypass duct exhaust.

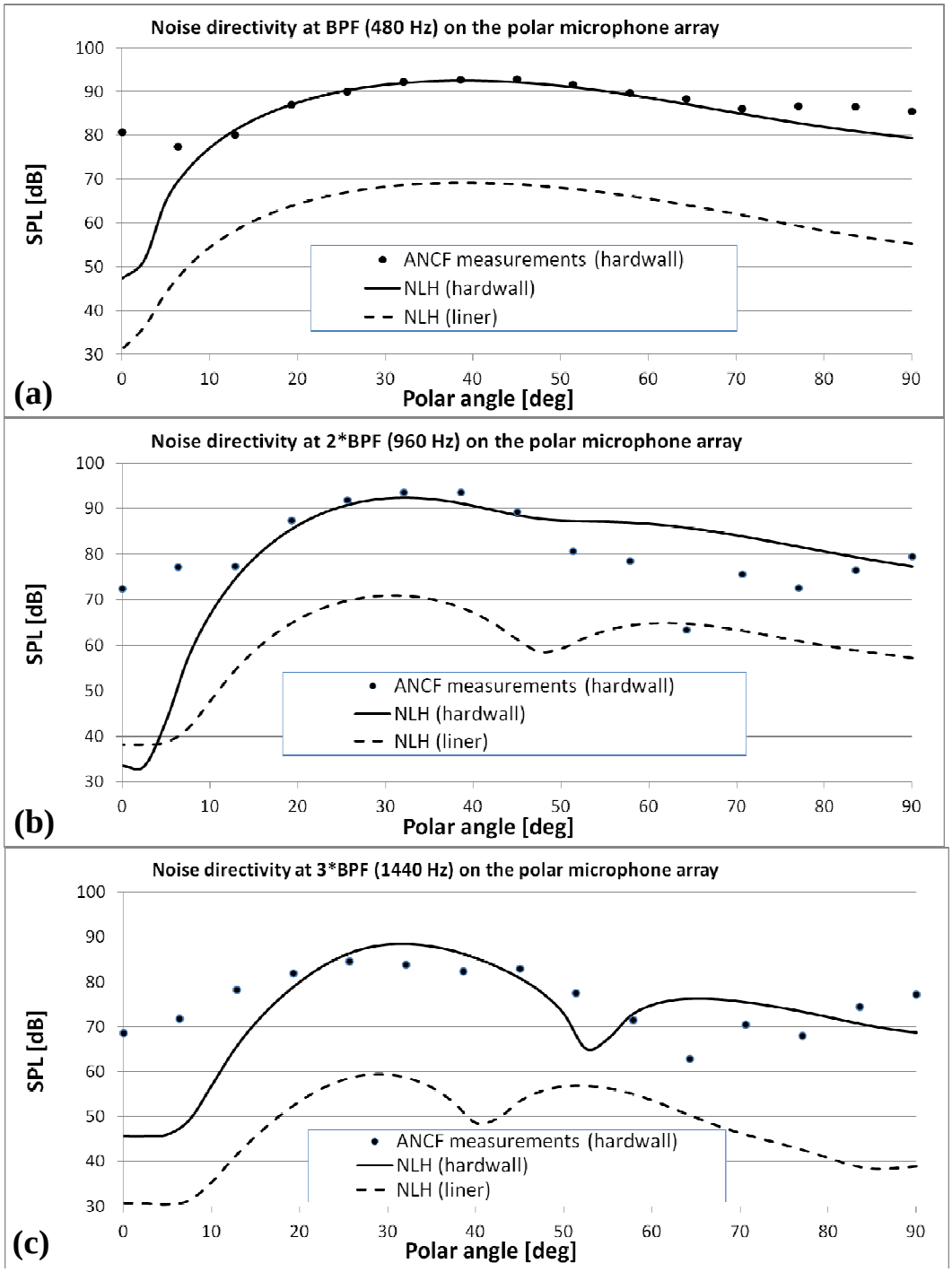

Figure 9: Noise directivity evaluated for the far-field microphones

The sound pressure levels are reduced by values of the order of 20 dB for the case with liner which is quite notable for a first simulation. However, as already mentioned, this liner is idealized since the damping is normally effective for one particular frequency with impedance values that depend on the frequencies. In the future, the goal will be to validate our methodology with experimental data from an actual acoustic liner in a nacelle turbofan.

CONCLUSIONS

An innovative integrated computational approach has been successfully applied to the simulation of acoustic liners for two test cases, for one of which experimental acoustic data are available. The simulation approach is based on the exploitation of an efficient CFD solver which implements the NLH method with acoustic liners for the simultaneous computation of the noise sources and its near-field propagation; coupled to a frequency domain aero-acoustic BEM solver, for the radiation analysis to the far-field.

The approach has been validated through various test cases, including a comparison with experimental results from the Grazing Incidence Tube at the NASA Langley Research Center. We compared the numerical results obtained from the Euler and Navier-Stokes solvers using the NLH method for a nominal impedance with the experimental data from Jones et al [6]. The results show that the methods are capable of predicting the effects of the liner quite well, with the Navier-Stokes solver giving in general more accurate results than the Euler solver.

The computational approach has also been applied to the simulation of the ANCF (Advanced Noise Control Fan) turbofan engine developed at the NASA Glenn Research Center. No experimental data were available to compare with for the case with liner and a constant impedance value representative of typical liner configurations installed in turbofan engine nacelles was applied. As expected, the presence of the liner considerably reduces the harmonic pressure fluctuations within the duct and in the near-field and reduces the sound pressure levels for the far-field directivities.

The integrated CFD-Acoustic approach presented in this study offers a fast, cheap and efficient simulation chain for the acoustic design of fans and turbofan engines incorporating acoustic liners. The proposed methodology can be effectively used in an industrial environment for optimization and design purposes. Such optimization tools have already been developed in the software FINE^{TM}/Turbo and they will be exploited to improve the shape and impedance values of acoustic liners.

ACKNOWLEDGEMENTS

The authors wish to thank Michael G. Jones for the measurements of the NASA Grazing Incidence Tube. The authors also express their gratitude to Daniel L. Sutliff of NASA Glenn Research Center for providing the ANCF geometry and the relative experimental database.

REFERENCES

[1] Ferrante, P., di Francescantonio, P., Hoffer, P.-A., Vilmin, S., Hirsch, Ch., (2014), “Integrated CFD-Acoustic computational approach to the simulation of aircraft fan noise”, ASME Turbo Expo 2014, GT2014-26429, Düsseldorf, Germany.

[2] Astley, R. J., Sugimoto, R., Mustafi, P., (2011), “Computational aero-acoutics for fan duct propagation and radiation. Current status and application to turbofan liner optimisation”, *Journal of Sound and Vibration*, 330, 3832-3845.

[3] Ingard, U., (1959), “Influence of fluid motion past a plane boundary on sound reflection, absorption, and transmission”, *Journal of the Acoustical Society of America*, 31 (7), 1035-1036

[4] Myers, M. K., (1980), “On the acoustic boundary condition in the presence of flow”, *Journal of Sound and Vibration*, 71 (3), 429-434.

[5] Burak, M. O., Billson, M., Eriksson, L.-E., Baralon, S., (2009), “Validation of a time- and frequency-domain grazing flow acoustic liner model”, *AIAA Journal*, 47 (8), 1841-1848.

[6] Jones, M. G., Watson, W. R., Parrott, T. L., (2005), “Benchmark data for evaluation of aeroacoustic propagation codes with grazing flow”, AIAA Paper No. 2005-2853, 11th AIAA/CEAS Aeroacoustics Conference, Monterey, CA.

[7] Loew, R.A., Lauer, J.T., McAllister J., Sutliff, D.L., (2006), “The advanced noise control fan”, AIAA Paper No. 2006-3150, also NASA TM-2006-214368.

[8] McAllister, J., Loew, R.A., Lauer, J.T., Sutliff, D.L., (2009), “The advanced noise control fan baseline measurements”, AIAA Paper No. 2009-0624.

[9] Vilmin, S., Lorrain, E., Hirsch, Ch., Swoboda, M., (2006), “Unsteady flow modeling across the rotor/stator interface using the nonlinear harmonic method”, ASME Turbo Expo 2006, GT2006-90210, Barcelona, Spain.

[10] He, L., and Ning, W., (1998), “Efficient approach for analysis of unsteady viscous flows in turbomachines”, *AIAA journal*, Vol. 36 (11), 2005-2012.

[11] Purwanto, A., Deconinck, T., Vilmin, S., Lorrain, E., Hirsch, C., (2011), “Efficient prediction of nacelle installation effects at take-off conditions”, ETC-9, Paper No 316.

[12] Vilmin, S., Lorrain, E., Debrabandere, F., Tartinville, B., Capron, A., Hirsch, Ch., (2013), "The nonlinear harmonic method applied to the combined effects of multi-row unsteady flows", ASME Paper No. GT2013-94847.

[13] di Francescantonio, P., (2008), “An efficient distributed BEM solver for acoustic and vibroacoustic analyses on a standard PC network”, *Journal of the Acoustical Society of America*, 123 (5), 3419-3419.

[14] A.D. Pierce, (2008), “Wave equation for sound in fluids with unsteady inhomogeneous flow”, *Journal of the Acoustical Society of America*, 87 (6), 2292-2299.

[15] di Francescantonio, P., (1997), “A new boundary integral formulation for the prediction of sound radiation”, *Journal of Sound and Vibration*, 202 (4), 491-509.

[16] Deconinck, T., Capron, A., Barbieux, V., Hirsch, C., Ghorbaniasl, G., (2011), “Sensitivity study on computational parameters for the prediction of noise generated by counter-rotating open rotors”, AIAA Paper No. 2011-2765, 17th AIAA/CEAS Aeroacoustics Conference, Portland, OR.

[17] Achunche, I., Astley, J., Sugimoto, R., and Kempton, A., (2009), “Prediction of forward fan noise propagation and radiation from intakes”, *AAIA Journal*, AIAA 2009-3239.

[18] Rossikhin, A., Pankov, S., Brailko, I., and Mileshin, V., (2014), “Numerical investigation of high bypass ratio fan tone noise”. ASME Turbo Expo 2014-26354, Düsseldorf, Germany.